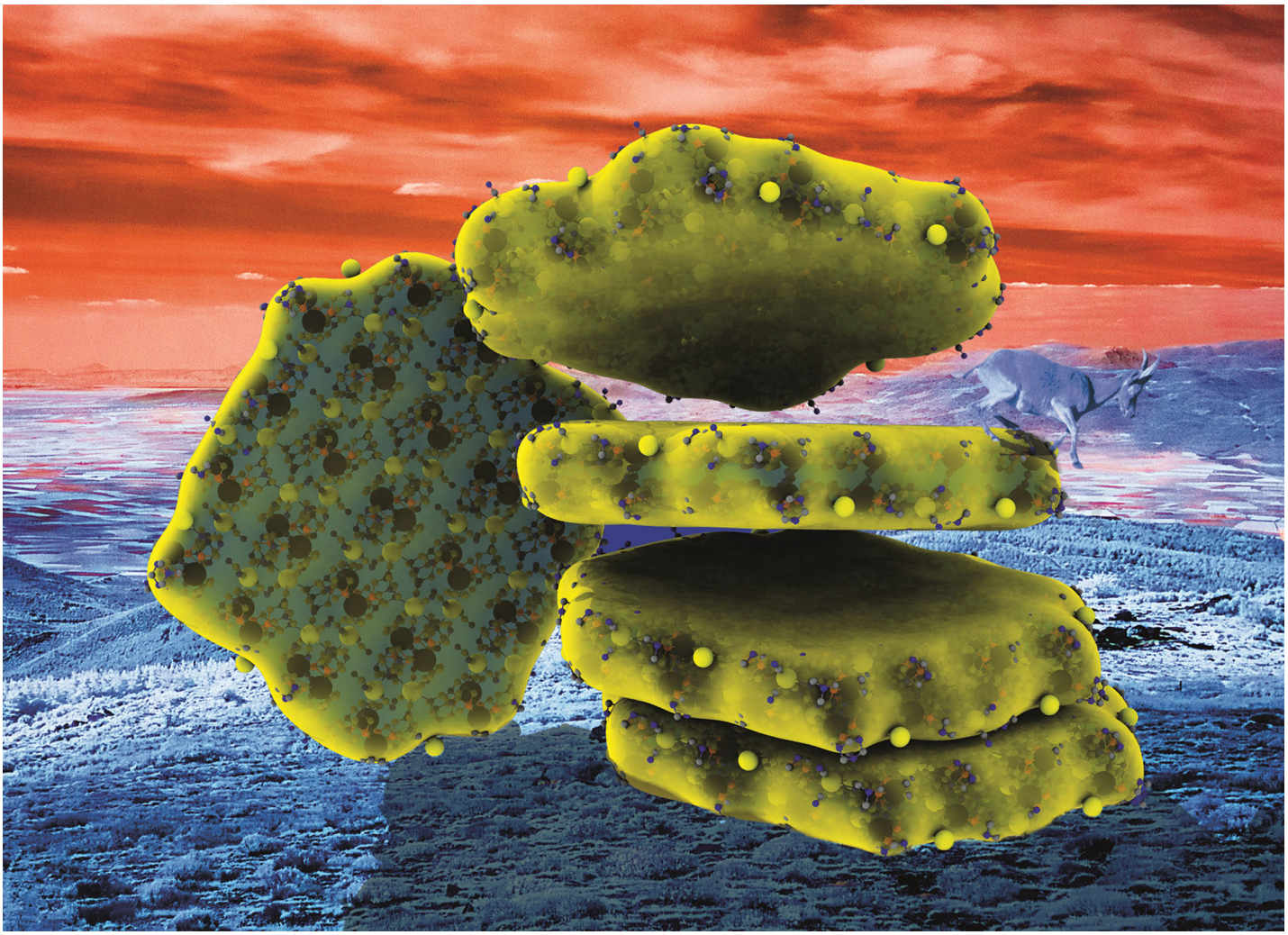

Showcasing research from Professor Romerosa's laboratory, Department of Chemistry and Physics, University of Almería, Almería, Spain. This illustration is designed by Franco Scalambra.

First exfoliated Ru–Ru–Au organometallic polymer with layered structure

Organometallic single layers of the robust Ru–Ru–Au polymer $[\{(PTA)_2CpRu\text{-}\mu\text{-}CN\text{-}1\kappa C{:}2\kappa^2 N\text{-}RuCp(PTA)_2\}\text{-}\mu\text{-}\{Au(CN)_4\}_4]_n \cdot 2H_2O$ can be easily obtained by its exfoliation in water. This complex self-assembles forming 3D polymeric structures with large scale hexagonal conformation organized as 3D stacks of polymer sandwiches that can be exfoliated.

As featured in:

See Antonio Romerosa *et al.*, *Chem. Commun.*, 2020, **56**, 9441.

ROYAL SOCIETY OF CHEMISTRY

rsc.li/chemcomm

Registered charity number: 207890

ChemComm

COMMUNICATION

Cite this: *Chem. Commun.*, 2020, **56**, 9441

Received 22nd June 2020,
Accepted 2nd July 2020

DOI: 10.1039/d0cc04325g

rsc.li/chemcomm

First exfoliated Ru–Ru–Au organometallic polymer with layered structure†

Franco Scalambra, [ab] Benjamin Sierra-Martin, [a] Manuel Serrano-Ruiz, [a] Antonio Fernandez-Barbero [ac] and Antonio Romerosa *[ab]

A new water soluble heterometallic polymeric complex [{(PTA)$_2$CpRu-μ-CN-1κC:2κ^{2}N-RuCp(PTA)$_2$}-μ-{Au(CN)$_4$}$_4$]$_n$·2H$_2$O (1) is synthesized and characterized by single crystal X-ray diffraction. This complex self-assembles forming 3D polymeric structures with large scale hexagonal conformation. They also organize as 3D stacks of polymer sandwiches that can be exfoliated providing mono heterometallic-3D layers, as shown by electron microscopy. Regarding the polymer dynamics, quasi-elastic neutron scattering shows a transition from vibrational Debye–Waller behaviour to a more dynamically active state as a result of the loss of structural water molecules.

Obtaining reproducible methods to achieve a controlled self-organization of molecules to form polymers and homo- or heterometallic aggregates is a matter of great interest in the field of coordination chemistry.[1–10] The first air-stable water soluble poly-metallic polymer with a mixed P,N ligand as a metal coordinating spacer was reported in a previous paper.[11] It consists of two metal-containing moieties, {CpRu}$^+$ and {AgCl$_2$}$^-$, bridged by the cage-like hydrophile monodentate phosphine PTA (PTA = 1,3,5-triaza-7-phosphaadamantane), in an unprecedented P,N coordinating mode. Metal polymers containing PTA are potential candidates for a variety of applications such as magnetism,[12] nonlinear optics,[13] electrocatalysis,[14] photocatalysis,[15] photovoltaics,[16] template formation of ordered networks,[17] advanced electrode materials,[18] and conjugated coordination polymers.[19]

After a considerable effort, the synthesis of analogue complexes with the general formula Na[RuCpX(PTA)-μ-(PTA)-1κP:2κ^{2}N-AgX$_2$]$_\infty$ (X = Cl, Br, I) was achieved and their novel gel properties reported.[20] A water-soluble and air-stable heterometallic polymer [{(PTA)$_2$CpRu-μ-CN-RuCp(PTA)$_2$}-μ-Au(CN)$_4$]$_n$, with a metal different to Ag was also obtained.[21] In addition, new Ru–Ru–M polymers with general formula [{RuCp(PTA)$_2$-μ-CN-1κC:2κ^{2}N-RuCp(PTA)$_2$}-μ-MX$_m$]$_n$ (M = transition metal; X = halide, pseudohalide) were incorporated to this family: [{RuCp(PTA)$_2$-μ-CN-1κC:2κ^{2}N-RuCp(PTA)$_2$}-μ-NICl$_3$]$_n$[22] and [{RuCp(PTA)$_2$-μ-CN-1κC:2κ^{2}N-RuCp(PTA)$_2$}-μ-CdCl$_2$]$_n$.[23] These polymers display properties not observed before for organometallic complexes such as the gelification in the presence of water[24] and the confinement of structural water into nano-channels.[25] Additional features, including crystallinity, make these polymers a brand new class of materials lying between metal organic frameworks (MOFs) and infinite coordination polymers (ICPs).[26]

Until now, the synthesis of the first 1D-Ru–Ru–Au complex was accomplished by the crystallization of a yellow powder obtained by reaction of [RuClCp(PTA)$_2$] with KCN and a solution of K[Au(CN)$_4$] in water.[21] This procedure is very sensitive to the reaction conditions and therefore appropriate only for microscale production. Further improvements, such as the use of the bimetallic complex [(PTA)$_2$CpRu-μ-CN-RuCp(PTA)$_2$](CF$_3$SO$_3$) as starting reagent, lead to the synthesis of polymeric materials containing [(PTA)$_2$CpRu-μ-CN-RuCp(PTA)$_2$]$^+$, linked by a variety of transition-metal complexes. The method was proven to be reproducible, robust and suitable to provide several grams of polymer. It also allows a fine control of the stoichiometry of reagents, which lead to new heterometallic polymers different to the known linear Ru–Ru–M.

In this paper we coordinate additional metallic species to the {(PTA)$_2$CpRu-μ-CN-RuCp(PTA)$_2$}$^+$ moiety through N centres, giving rise to a new Ru–Ru–Au organometallic polymer. This product is obtained by reacting [(PTA)$_2$CpRu-μ-CN-RuCp(PTA)$_2$]-(CF$_3$SO$_3$) with 5 equivalents of K[Au(CN)$_4$] in water (Scheme 1). Slow crystallization of the obtained yellow powder in H$_2$O/DMSO (under air) yield to yellow-orange single crystals suitable for single crystal X-ray diffraction. The complex presents a layered structure that can be exfoliated in ultrathin 3D layers, in a similar way to ruthenium-based metal–organic frameworks[27] and some metal oxides.[28,29]

[a] *Department of Chemistry and Physics, University of Almeria, 04120 Almeria, Spain. E-mail: romerosa@ual.es*
[b] *Inorganic Chemistry Lab-CIESOL, University of Almeria, 04120 Almeria, Spain*
[c] *Institute of Applied Chemical Sciences, Universidad Autonoma de Chile, 8320000 Santiago, Chile*

† Electronic supplementary information (ESI) available. CCDC 2002761. For ESI and crystallographic data in CIF or other electronic format see DOI: 10.1039/d0cc04325g

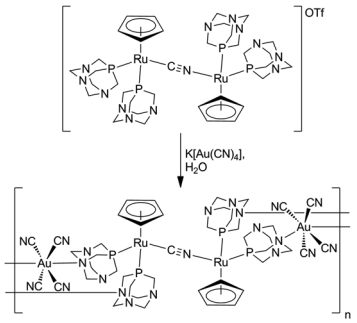

Scheme 1 Synthesis of **1**.

The complex is stable under air for months, insoluble in organic solvents but slightly soluble in polar solvents such as DMSO and water (0.8 mg mL^{-1}), remaining stable for more than two days under air in water. Nevertheless, this polymer partially decomposes when solubilized in water, releasing $\{(PTA)_2CpRu\text{-}\mu\text{-}CN\text{-}RuCp(PTA)_2\}^+$ cations and forming polydisperse microparticles, as determined by dynamic light scattering (see ESI†). The 99.9% in volume of microparticles is distributed within two main average size ranges (diameter): 107 ± 43 nm and 332 ± 131 nm. Additionally, a residual population was detected at 4098 ± 1175 nm, corresponding to 0.1% in volume. These results are consistent with the colloidal size previously reported for Ru–Ru–Au polymer.[21] Considering that particles with diameter >0.22 μm were filtered prior to the DLS measurement, the presence of large particles may be related to a self-aggregation mechanism.

The asymmetric unit in the crystal structure is constituted by two water molecules, a $\{Au(CN)_4\}^-$ complex unit and half molecule of binuclear cationic complex $\{(PTA)_2CpRu\text{-}\mu\text{-}CN\text{-}RuCp(PTA)_2\}^+$, where two piano-stool $\{CpRu(PTA)_2\}^+$ moieties are linked by a disordered CN^- ligand (50%). Growing of the asymmetric unit leads to a polymer in which the four PTA ligands are coordinated by a N atom to a $\{Au(CN)_4\}$ moiety, as shown in Fig. 1. Bond lengths and angles of the polymer complex **1** are provided in the Supporting Information. The crystal structure of the starting dimeric Ru–Ru moiety is similar to that of the 1D-parent polymer $[\{(PTA)_2CpRu\text{-}\mu\text{-}CN\text{-}RuCp(PTA)_2\}\text{-}\mu\text{-}Au(CN)_4]_n$.[24] Both Cp and PTA ligands points out to opposite directions due to an inversion centre located on the CN bridging ligand. The interatomic distances in the dimeric Ru–CN–Ru moiety are similar to those in the dimeric complex[30] (**1**: Ru–CNC(CNC) = 2.012(3) Å; CNC≡NCN = 1.151(5) Å. dimeric $[CpRu(PTA)_2\text{-}\mu\text{-}CN\text{-}(PTA)_2RuCp]^+$ complex: Ru–CN(NC) = 2.012(5) Å; C≡N = 1.137(9) Å; Ru–CN(NC) = 2.028(5) Å; C≡N = 1.151(10) Å). The Ru–CN–Ru bond lengths in **1** are similar to those found for Cp-ruthenium complexes containing coordinate CN^-[31] and for the complex $\{[\{(PTA)_2CpRu\text{-}\mu\text{-}CN\text{-}RuCp(PTA)_2\}\text{-}\mu\text{-}Au(CN)_4]\}_n$ (Ru1–N1P = 2.027(3) Å, N1P–C1P = 1.152(6) Å).[24]

The Au–CN distances are very close to each other (1.995(3) Å–2.006(3) Å: average: 2.002 Å) and also similar to that found for the 1D-polymer (1.999 Å), falling into the literature limits for Au–CN distances.[24] The bond distances of the Au with the PTA-N

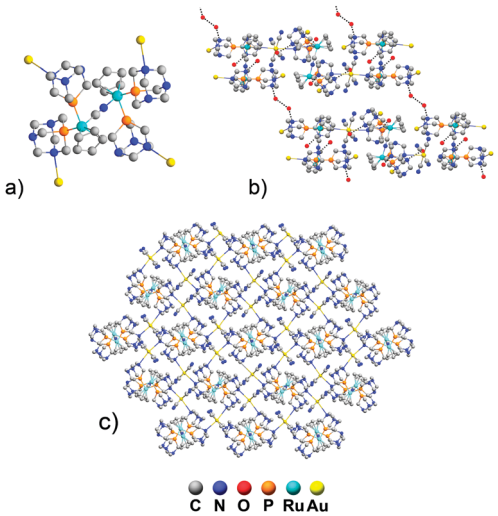

Fig. 1 (a) Representation of the Au centres coordinated around the $[(PTA)_2CpRu\text{-}\mu\text{-}CN\text{-}RuCp(PTA)_2]^+$ moiety in **1**. (b) Side view of two adjacent hydrogen bonded layers of **1**; the polymeric layers are connected *via* N4···O2W···O2W···N4 hydrogen bonds, forming single layers packed in a sandwich-like manner. (c) Top view of a single layer of **1** in the crystal structure. The hydrogen atoms were omitted for clarity.

($Au\text{–}N_{PTA}$) are longer (Au1–N1 = 2.952(2) Å; Au1–N6 = 3.193(3) Å) than the corresponding to others diamino–Au complexes (2.13 Å). They are similar to that found for 1D-Ru–Ru–Au polymers (2.985(3) Å) and shorter than the sum of the van der Waals radii for Au and N (3.21 Å).[32] The coordination geometry around the Au metal atom in **1** (C1G–Au1–N6 = 79.72°) is more distorted compared to the 1D-Ru–CN–Ru–Au polymer (C2C–Au1–N3 = 96.55°). This fact indicates a larger structural tension due to coordination of the four Au atoms to the $\{Cp(PTA)_2Ru\text{–}CN\text{–}Ru(PTA)_2Cp\}^+$ moiety. We note that this is the second example of a crystallographically authenticated octahedral Au complex containing cyano-ligands.[22] Interestingly, the polymer packs in a 3D layer where $\{Cp(PTA)_2Ru\text{–}CN\text{–}Ru(PTA)_2Cp\}^+$ dimers constitute the thickness of the layer and $\{AuCN_4\}^-$ moieties link them along the structure. Each layer is connected to the adjacent one by water molecules bridging them *via* hydrogen bonds with N_{PTA} atoms of vicinal molecules (N4–O2W = 2.754(4) Å; O2W–O2W = 2.684(4) Å) (Fig. 1).

The IR spectra of **1** shows ν(Ru–CN) and ν(Au–CN) absorption bands at 2094 cm^{-1} and 2183 cm^{-1}, similarly to that in complex 1D-Ru–Ru–Au (ν(Ru–C≡N) = 2097 cm^{-1}; ν(Au–C≡N) = 2185 cm^{-1}).[24] The ν(Ru–C≡N) is also similar for complexes Ru–CN–Ru–Ni (2107 cm^{-1}) and $[CpRu(PTA)_2\text{-}\mu\text{-}CN\text{-}Ru(PTA)_2Cp]^+$ (2113 cm^{-1}), and larger than complex $[RuCp(CN\text{-}\kappa C)(PTA)_2]$ (2060 cm^{-1}). The absorption of bridging cyano-groups agrees with that for similar bi-nuclear cyano-complexes.[33,34] Polymer complex **1** is characterized by two singlet signals at −19.33 (PTA-Ru-N) and −21.95 (PTA-Ru-C) in $^{31}P\{^1H\}$ NMR (D_2O), close to that observed for the polymer Ru–CN–Ru–Au (−19.21 and −21.82 ppm) and the dimeric complex $[(PTA)_2CpRu\text{-}\mu\text{-}CN\text{-}RuCp(PTA)_2](CF_3SO_3)$. This behaviour is analogous to that observed in linear Ru–CN–Ru–M polymers. These complexes in water are shortly in equilibrium with $[(PTA)_2CpRu\text{-}\mu\text{-}CN\text{-}RuCp(PTA)_2]^+$, being most of the complex

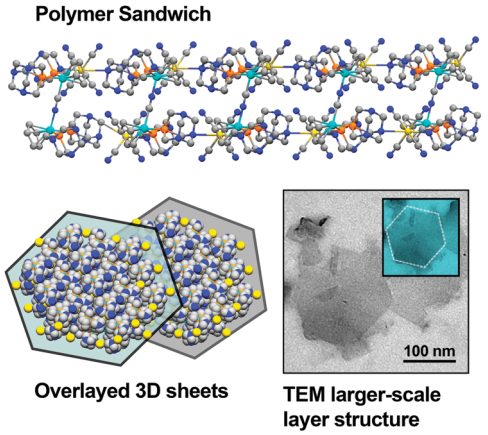

Fig. 2 Representation of the polymer sandwich from the side and from the top. Transmission electron microscopy showing hexagonal structures at larger dimensional scale.

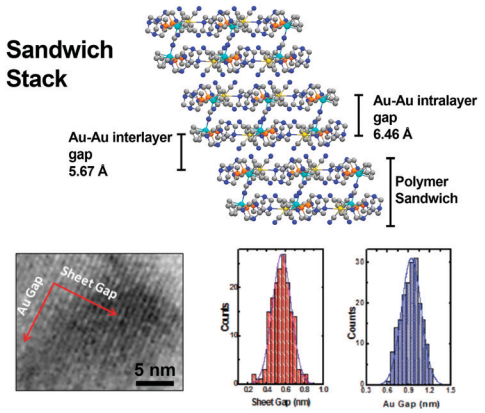

Fig. 3 3D polymer sandwich stacks. Structure projection from top. HRTEM picture showing stripes corresponding to different layers in the stack. Probability distributions for the interlayer gaps and distances between adjacent gold atoms in the structure.

in the form of a gel. The ^{1}H NMR spectrum has proven to be consistent with this finding. The thermo-gravimetric analysis of the polymer (see ESI†) shows that four interstitial water molecules are lost in two different and partially overlapped processes (three H_2O at 56.8 °C; one H_2O at 82.6 °C) with offset at 160 °C.

Fig. 2 shows a sketch of the sandwich-layered polymer structure (upper part). At the left down corner, a 2D projection from top is shown. At higher dimensional scale, the polymer sandwiches structure into hexagonal stable sheets that can be separated in water at room temperature by exfoliation in an ultrasonic bath. Transmission electron microscopy shows two semi-overlapped sheets with hexagonal contour (the upper inset is a guide to the eye to stand the geometric shape out). Several attempts with atomic force microscopy were performed to determine the thickness of the polymer sandwich. Unfortunately, it could not be determined with sufficient accuracy for conclusions. High resolution transmission electron microscopy was then used as alternative technique. TEM micrographs were taken with a JEOL JEM 2100 high resolution electron microscope through the perpendicular direction to the layered structure. It allows estimating the polymer sandwich thickness as well as the gap between different polymer sandwiches.

Fig. 3 shows a set of stripes corresponding to a stack of polymer in which the distances between layers are determined by analysing the grey intensity profiles along a path perpendicular to the stripes. Statistics is performed by computing a set of different paths. The Gaussian curve represents the frequency of finding a specific distance between stripes. The maximum probability corresponds to a distance of about 0.6 nm. This value is consistent with the distance estimated by X-ray diffraction (0.6428 nm for the polymer sandwich thickness and 0.5626 nm for the inter-sandwich gap). The second Gaussian curve is the distance between gold atoms, recorded by walking along one stripe. The maximum probability of finding two gold contiguous atoms is located about 0.9 nm, which is of the order of the distances determined by X-ray (1.0086 nm and 1.1252 nm).

The polymer dynamics was studied through incoherent quasielastic neutron-scattering experiments at the IRIS time-of-flight instrument (Rutherford Appleton Laboratory, ISIS Facility).[35] The instrument allows to observe relaxations within a distribution of energies in the range of μeV, arising from rotations, translations, *etc.* The inset on Fig. 4a illustrates the dynamic structure factors at $Q = 1.36$ Å^{-1}, recorded for different temperatures. Spectra are normalized to its maximum elastic value to praise the widths broadening. The incoherent scattering function may be written as $S(Q, \omega) = R(Q, \omega) \otimes [\delta(\omega) + L(Q, \omega)]$, with $L(Q,\omega) = \pi^{-1}[\Gamma(Q)/(\pi\omega^2 + \Gamma^2(Q))]$. $R(Q, \omega)$ is the resolution function of the instrument and BG is the constant background. The delta function $\delta(\omega)$ is attributed to the static component (motion much slower than instrumental resolution) mainly from hydrogen atoms and slightly from the coherent scattering contribution from other atoms. $L(Q, \omega)$ describes the hydrogen atoms relaxation. For typical Debye relaxation (exponential decay), $L(Q, \omega)$ is expressed by a Lorentz function. $\Gamma(Q)$ is the half width at half maximum (FWHM).

Fig. 4a shows $\Gamma(Q)$ broadening for increasing temperatures recorded at $Q = 1.36$ Å^{-1}, consistent with Debye–Waller. At ~300 K, the polymer becomes softer due to the loss of structural water

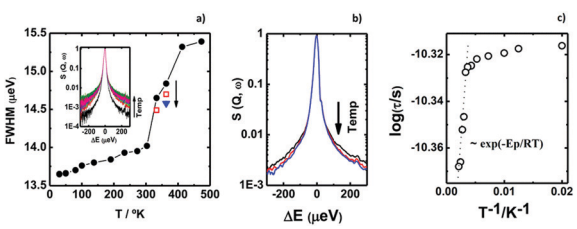

Fig. 4 (a) ●: FWHM of the first heating half-cycle (from 30.15 K to 473.15 K, first time). □: FWHM at 333 K and 363 K for the second up-heating cycle (after the first [30 K–473 K–30 K] cycle). ▼ FWHM at 333 K and 363 K for the third up-heating cycle (after twice [30 K–473 K–30 K] cycles). Inset: Scattering curves for the first heating half-cycle. (b) Scattering curves for the up-heating second and third cycles, corresponding to the observed hysteresis. (c) Arrhenius-type plot. The sharp region corresponds to an exponential relaxation, with E_a being the activation energy.

(by temperature increasing) and the chain translational diffusion increases. In order to reinforce this explanation, several heating and cooling cycles were performed. It is observed an irreversible decrease in the FWHM values, which is attributed to progressive loss of structural water. Fig. 4b plots the spectra corresponding to the three experiments showing the irreversibility. The temperature influence on the relaxation time, $\tau = 1/\Gamma$, is evaluated from the Lorentz fit[36] and plotted in Fig. 4c. Data lying on a straight line leads to an Arrhenius-type relaxation. The activation Energy ΔE_a is obtained from the slope of $\log \tau = \log \tau_0 + \Delta E_a/RT$, with R (=8.314 J K^{-1} mol^{-1}) being the gas constant and τ_0 the relaxation time at very large temperature. The activation energy was found to be 0.26 kJ mol^{-1}. This relaxation is associated to the motion of the hydrogen attached to the PTA and Cp units.[24]

We have reported the synthesis of a novel Ru–Ru–Au heterometallic polymer complex with formula $[\{(PTA)_2CpRu\text{-}\mu\text{-}CN\text{-}1\kappa C{:}2\kappa^2 N\text{-}RuCp(PTA)_2\}\text{-}\mu\text{-}\{Au(CN)_4\}_4]_n \cdot 2H_2O$. The polymer self-assembles in 3D layers with large scale hexagonal conformation. They also organize as 3D stacks of polymer sandwiches. The layered structure can be exfoliated in a similar way than graphene sheets, which open promising applications. Isolated monolayers or a bunch of pilled layers containing different metals in defined positions could display different optical, electrical or catalytic properties. Quasi-elastic neutron scattering gives some insights on the changes of the polymer dynamics, indicating the structural stability of the compound in solid state. A transition from vibrational Debye–Waller to a more dynamically active state results from the loss of structural water, with no decomposition of the structure. More efforts are being conducted to establish a robust procedure for obtaining complex **1** in a defined number of layers, where physical and chemical properties could be assessed.

Authors acknowledge the support of Project CTQ2015-67384-R, CTQ2017-90050-R (MINECO/FEDER). AFB thanks support from Institute of Applied Chemical Sciences, Universidad Autonoma de Chile. Thanks are also given to actions by Junta de Andalucia (PAI research teams FQM-317). We acknowledge the beamtime awarded at the ISIS Neutron and Muon source. We also thanks to A. Camara et al. for L-S measurements.

Conflicts of interest

There are no conflicts to declare.

Notes and references

1 *Frontiers in Transition Metal-Containing Polymers*, ed. I. M. Alaa and S. Abd-El-Aziz, Wiley VCH, Hoboken, 2007.
2 M. Serrano-Ruiz, F. Scalambra and A. Romerosa, in *Advances in Organometallic Chemistry and Catalysis*, ed. A. J. L. Pombeiro, Wiley VCH, 2013, pp. 381–407.
3 J. C. Eloi, L. Chabanne, G. R. Whittell and I. Manners, *Mater. Today*, 2008, **11**, 28–36.
4 J. M. Lehn, *Supramolecular Chemistry: Concepts and Perspectives*, ed J. M. Lehn, John Wiley & Sons Ltd, 1995.
5 K. A. Williams, A. J. Boydston and C. W. Bielawski, *ChemInform*, 2007, **36**(5), 729–744.
6 M. Eddaoudi, D. B. Moler, H. Li, B. Chen, T. M. Reineke, M. O'Keeffe and O. M. Yaghi, *Acc. Chem. Res.*, 2001, **34**(4), 319–330.
7 S. Leininger, B. Olenyuk and P. J. Stang, *Chem. Rev.*, 2000, **100**(3), 853–908.
8 D. L. Caulder and K. N. Raymond, *Acc. Chem. Res.*, 1999, **32**(11), 975–982.
9 D. Braga, F. Grepioni and G. R. Desiraju, *Chem. Rev.*, 1998, **98**(4), 1375–1406.
10 P. J. Stang and B. Olenyuk, *Acc. Chem. Res.*, 1997, **30**(12), 502–518.
11 C. Lidrissi, A. Romerosa, M. Saoud, M. Serrano-Ruiz, L. Gonsalvi and M. Peruzzini, *Angew. Chem., Int. Ed.*, 2005, **44**, 2568–2572.
12 J. S. Miller, *Inorg. Chem.*, 2000, **39**(20), 4392–4408.
13 *Optoelectronic Properties of Inorganic Compounds*, ed. F. Roundhill, D. M., Fackler, J. P., Jhon, Plenum Press, New York, 1999.
14 R. P. Kingsborough and T. M. Swager, *Chem. Mater.*, 2000, **12**(4), 872–874.
15 W. K. Chan, in *Macromolecules Containing Metal and Metal-Like Elements: Metal-Coordination Polymers*, ed. M. Abd-El-Aziz, A. S. Carraher, C. E. Pittman, C. U. Zeldin, John Wiley & Sons, Inc, vol. 5, 2005.
16 K. C. Wai, C. S. Hui, K. Y. K. Man, W. C. Kai, L. W. Hei, N. Zhu and A. B. Djurišić, *Coord. Chem. Rev.*, 2005, **249**(13–14), 1351–1359.
17 A. Kokil, P. Yao and C. Weder, *Macromolecules*, 2005, **38**(9), 3800–3807.
18 J. Roncali, *J. Mater. Chem.*, 1999, **9**, 1875–1893.
19 D. Knapton, S. J. Rowan and C. Weder, *Macromolecules*, 2006, **39**(2), 651–657.
20 B. Sierra-Martín, M. Serrano-Ruiz, F. Scalambra, A. Fernandez-Barbero and A. Romerosa, *Polymers*, 2019, **11**, 1249.
21 M. Serrano Ruiz, A. Romerosa, B. Sierra-Martin and A. Fernandez-Barbero, *Angew. Chem., Int. Ed.*, 2008, **47**, 8665–8669.
22 F. Scalambra, M. Serrano-Ruiz and A. Romerosa, *Macromol. Rapid Commun.*, 2015, **36**, 689–693.
23 F. Scalambra, M. Serrano-Ruiz, D. Gudat and A. Romerosa, *ChemistrySelect*, 2016, **1**, 901–905.
24 B. Sierra-Martin, M. Serrano-Ruiz, V. García-Sakai, F. Scalambra, A. Romerosa and A. Fernandez-Barbero, *Polymers*, 2018, **10**(5), 528.
25 F. Scalambra, M. Serrano-Ruiz and A. Romerosa, *Dalton Trans.*, 2017, **46**, 5864–5871.
26 A. M. Spokoyny, D. Kim, A. Sumrein and C. A. Mirkin, *Chem. Soc. Rev.*, 2009, **38**, 1218.
27 D. Huo, F. Lin, S. Chen, Y. Ni, R. Wang, H. Chen, L. Duan, Y. Ji, A. Zhou and L. Tong, *Inorg. Chem.*, 2020, **59**(4), 2379–2386.
28 S. Wang, S. Li, R. Shi, X. Zou, Z. Zhang, G. Fu, L. Li and F. Luo, *Dalton Trans.*, 2020, **49**, 2559–2569.
29 Q. Zeng, L. Wang, Y. Huang, S. L. Zheng, Y. He, J. He, W. M. Liao, G. Xu, M. Zeller and Z. Xu, *Chem. Commun.*, 2020, **56**, 3645–3648.
30 D. N. Akbayeva, L. Gonsalvi, W. Oberhauser, M. Peruzzini, F. Vizza, P. Brüggeller, A. Romerosa, G. Sava and A. Bergamo, *Chem. Commun.*, 2003, 264–265.
31 Cambridge Structural Database (CDS): http://www.ccdc.cam.ac.uk/products/csd/.
32 F. Romerosa and A. Scalambra, in *Non-covalent Interactions in the Synthesis and Design of New Compounds*, ed. A. J. L. P. A. M. Maharramov, K. T. Mahmudov and M. N. Kopylovich, Wiley VCH, Hoboken, 2016, 85–89.
33 G. J. Baird, S. G. Davies, S. D. Moon, S. J. Simpson and R. H. Jones, *J. Chem. Soc., Dalton Trans.*, 1995, **7**, 1479–1486.
34 G. E. Pieslinger, P. Albores, L. D. Slep, B. J. Coe, C. J. Timpson and L. M. Baraldo, *Inorg. Chem.*, 2013, **52**(6), 2906–2917.
35 ISIS Muon and Neutron Source: IRIS, https://www.isis.stfc.ac.uk/Pages/iris.aspx.
36 M. Kofu, T. Someya, S. Tatsumi, K. Ueno, T. Ueki, M. Watanabe, T. Matsunaga, M. Shibayama, V. G. Sakai, M. Tyagi and O. Yamamuro, *Soft Matter*, 2012, **8**, 7888.

